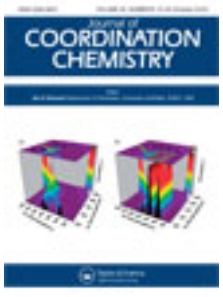

Journal of Coordination Chemistry
Publication details, including instructions for authors and subscription information:
http://www.tandfonline.com/loi/gcoo20

Synthesis, crystal structure, and catalytic performance of two 3-D supramolecular compounds: $(C_7N_2H_7)_3(C_7N_2H_6)\cdot PMo_{12}O_{40}\cdot 2H_2O$ and $(C_7N_2H_7)_3(C_7N_2H_6)_2\cdot AsMo_{12}O_{40}\cdot 3H_2O$

Qian Deng [a], Chuan-Lei Zhang [a], Jian-Ting Tang [a], Shu-Zi Lü [a], Hong-Li Ma [a] & Tie-Jun Cai [a]

[a] Key Laboratory of Theoretical Chemistry and Molecular Simulation of Ministry of Education, Hunan University of Science and Technology, Xiangtan 411201, China

Accepted author version posted online: 27 Jul 2012.Published online: 22 Aug 2012.

To cite this article: Qian Deng, Chuan-Lei Zhang, Jian-Ting Tang, Shu-Zi Lü, Hong-Li Ma & Tie-Jun Cai (2012) Synthesis, crystal structure, and catalytic performance of two 3-D supramolecular compounds: $(C_7N_2H_7)_3(C_7N_2H_6)\cdot PMo_{12}O_{40}\cdot 2H_2O$ and $(C_7N_2H_7)_3(C_7N_2H_6)_2\cdot AsMo_{12}O_{40}\cdot 3H_2O$, Journal of Coordination Chemistry, 65:19, 3458-3468, DOI: 10.1080/00958972.2012.716515

To link to this article: http://dx.doi.org/10.1080/00958972.2012.716515

Journal of Coordination Chemistry
Vol. 65, No. 19, 10 October 2012, 3458–3468

Synthesis, crystal structure, and catalytic performance of two 3-D supramolecular compounds: $(C_7N_2H_7)_3(C_7N_2H_6)\cdot PMo_{12}O_{40}\cdot 2H_2O$ and $(C_7N_2H_7)_3(C_7N_2H_6)_2\cdot AsMo_{12}O_{40}\cdot 3H_2O$

QIAN DENG, CHUAN-LEI ZHANG, JIAN-TING TANG, SHU-ZI LÜ, HONG-LI MA and TIE-JUN CAI*

Key Laboratory of Theoretical Chemistry and Molecular Simulation of Ministry of Education, Hunan University of Science and Technology, Xiangtan 411201, China

(*Received 23 December 2011; in final form 14 May 2012*)

Two organic–inorganic compounds based on Keggin building blocks have been synthesized by hydrothermal methods, $(C_7N_2H_7)_3(C_7N_2H_6)\cdot PMo_{12}O_{40}\cdot 2H_2O$ (**1**) and $(C_7N_2H_7)_3(C_7N_2H_6)_2\cdot AsMo_{12}O_{40}\cdot 3H_2O$ (**2**) ($C_7N_2H_6$ = benzimidazole). Single-crystal X-ray analysis revealed that **1** crystallized in the triclinic system, *P*-1 space group with $a = 9.8980(4)$ Å, $b = 11.2893(4)$ Å, $c = 25.8933(9)$ Å, $\alpha = 93.307(2)^\circ$, $\beta = 90.630(2)^\circ$, $\gamma = 108.330(2)^\circ$, $V = 2740.68(18)$ Å^3, $Z = 2$, $R_1(F) = 0.0740$, $\omega R_2(F^2) = 0.1511$, and $S = 1.037$; **2** crystallized in the triclinic system, *P*-1 space group with $a = 12.3353(4)$ Å, $b = 13.2649(4)$ Å, $c = 20.2878(6)$ Å, $\alpha = 95.6630(10)^\circ$, $\beta = 100.1720(10)^\circ$, $\gamma = 99.3940(10)^\circ$, $V = 3195.72(17)$ Å^3, $Z = 2$, $R_1(F) = 0.0329$, $\omega R_2(F^2) = 0.1236$, and $S = 1.088$. The two compounds show a layer framework constructed from Keggin-polyoxoanion clusters and benzimidazole *via* hydrogen bonds and π–π stacking interactions, resulting in a 3-D supramolecular network. Both have high catalytic activity for oxidation of methanol. When the initial concentration of the methanol is 5.37 g m^{-3} in air and the flow velocity is 4.51 mL min^{-1}, methanol is completely eliminated at 150°C for **1** (160°C for **2**).

Keywords: Keggin-polyoxoanion; Hydrothermal technology; Supramolecular compounds; Methanol oxidation; Catalytic elimination

1. Introduction

Keggin-type polyoxometalates (POMs) $[XM_{12}O_{40}]^{n-}$ (X = B, P, Si, Ge, As) have received considerable attention in the past years due to their unusual electronic properties, interesting structural chemistry, and potential applications [1–5]. POMs, which are excellent molecular acceptors, can form complexes with a number of organic substrates containing N, S, and O. Many inorganic–organic hybrid compounds with optical properties including charge-transfer salts constructed from POMs and organic moieties were synthesized by molecular self-assembly for such as photochromism or nonlinear optics [6–9]. Synthesis of organic–inorganic hybrid POMs has become a focus

*Corresponding author. Email: tjcai53@163.com

ISSN 0095-8972 print/ISSN 1029-0389 online
http://dx.doi.org/10.1080/00958972.2012.716515

of contemporary research due to magnetic, electrical, and optical properties [10]. Shringarpure and Tripuramallu [11] reported the synthesis of cesium salt of mono-cobalt-substituted phosphotungstate ($PW_{11}O_{39}Co$), which was different from the two-step synthesis of cobalt-substituted phosphotungstate previously. Proton-conductive complexes have been reported by Wei [12], $\{[H(H_2O)_2][Sr(HINO)_4(H_2O)_7(PW_{12}O_{40})]\}_n$ and $\{[H(H_2O)_2][Ca(HINO)_4(H_2O)_5(PW_{12}O_{40})]\}_n$, both constructed by introducing alkaline-earth metal ions and $[PW_{12}O_{40}]^{3-}$ in H-bonding networks based on isonicotinic acid N-oxide (HINO).

Here, we report the hydrothermal synthesis, crystal structure, and catalytic properties of two new organic–inorganic POMs, $(C_7N_2H_7)_3(C_7N_2H_6)\cdot PMo_{12}O_{40}\cdot 2H_2O$ (**1**) and $(C_7N_2H_7)_3(C_7N_2H_6)_2\cdot AsMo_{12}O_{40}\cdot 3H_2O$ (**2**) ($C_7N_2H_6$ = benzimidazole). The compounds have a 3-D organic–inorganic supramolecule network along the *a*-axis through hydrogen bonds and π–π stacking interactions. Both exhibit high catalytic activities for oxidation of methanol tested in a continuous-flow fixed-bed micro-reactor.

2. Experimental

2.1. *Materials and general methods*

All chemicals (reagent grade) were commercially available and used without purification. Elemental analysis was performed using a Perkin-Elmer 2400 CHN elemental analyzer. Mo, As, and P were determined by a SHIMADZU ICP emission spectrometer. Infrared spectra in KBr pellets (4000–400 cm^{-1}) were recorded using a Perkin-Elmer FTIR-2000 spectrophotometer. Thermal analysis (TG-DTA) was carried out on a WCT-1D microcomputer differential thermal balance (Beijing Optical Instrument Factory, China) in air with a heating rate of 10°C min^{-1}. The products of the catalytic reaction were analyzed on-line by a GC-9800 gas chromatograph (GC) equipped with a column packed with Porapak-Q and using a flame ionization detector.

2.2. *Hydrothermal synthesis*

2.2.1. $(C_7N_2H_7)_3(C_7N_2H_6)\cdot PMo_{12}O_{40}\cdot 2H_2O$ (1). A mixture of $Na_3PO_4\cdot 12H_2O$ (0.3801 g, 1.0000 mmol), $Na_2MoO_4\cdot 2H_2O$ (2.9034 g, 12.0000 mmol), benzimidazole (0.1181 g, 1.0000 mmol), 1 : 1 H_2SO_4 (V : V 2.5 mL), and H_2O (50 mL) was stirred for 45 min. The solution was sealed in an 80 mL Teflon-lined bomb at 180°C for 120 h, then the autoclave was cooled at 10°C h^{-1} to room temperature. Dark brown block-like crystals were collected by filtration, washed by distilled water, and air-dried in a yield of 61% based on the initial benzimidazole. Anal. Calcd for $C_{28}H_{31}O_{42}N_8PMo_{12}$ (**1**) (%): C, 14.40; H, 1.33; N, 4.80; Mo, 49.36; P, 1.33. Found: C, 13.96; H, 1.32; N, 4.91; Mo, 49.88; P, 1.44.

2.2.2. $(C_7N_2H_7)_3(C_7N_2H_6)_2\cdot AsMo_{12}O_{40}\cdot 3H_2O$ (2). A mixture of $Na_3AsO_4\cdot 12H_2O$ (0.0848 g, 0.2000 mmol), $Na_2MoO_4\cdot 2H_2O$ (0.5808 g, 2.4000 mmol), benzimidazole (0.0236 g, 0.2000 mmol), 1 : 1 H_2SO_4 (V : V, 1 mL) and H_2O (15 mL) was sealed in a 25 mL Teflon-lined bomb at 180°C for 120 h, then the autoclave was cooled at 10°C h^{-1}

to room temperature. Red block-like crystals were collected by filtration, washed by distilled water, and air-dried in a yield of 53% based on the initial benzimidazole input. Anal. Calcd for $C_{35}H_{39}AsMo_{12}N_{10}O_{43}$ (**2**) (%): C, 16.71; H, 1.55; N, 5.57; Mo, 45.79; As, 2.98. Found: C, 16.53; H, 1.48; N, 5.70; Mo, 45.91; As, 2.83.

2.3. *X-ray crystallography*

Suitable crystals of **1** and **2** were selected for lattice parameter determination and collection of intensity data at 293(2) K on a Bruker SMART Apex II CCD area detector single-crystal diffractometer with graphite-monochromated Mo-Kα radiation ($\lambda = 0.71073$ Å) using φ–ω scans. Absorption correction was applied using SADABS [13]. The structure was solved with direct methods using SHELXS-97 [14] and refined by full matrix least-squares on F^2 (SHELXL-97 [15]). All hydrogen atoms were generated geometrically. All non-hydrogen atoms were refined with anisotropic displacement parameters, and hydrogen atoms with isotropic displacement parameters. Further information about the crystal data and structure determination is summarized in table 1. Selected interatomic distances and angles are given in tables 2 and 3. CCDC reference numbers are 821843 for **1** and 819061 for **2**.

2.4. *Catalytic reaction for methanol elimination*

The catalytic elimination of methanol was used as a model reaction to evaluate the catalytic performances of **1** and **2**. Catalytic reactions were carried out in a continuous-flow fixed-bed micro-reactor (Supplemental material). 0.20 g of **1** (or **2**) was loaded in the catalytic reaction tube ($\varphi = 8$ mm; $L = 200$ mm) as a catalyst.

The simulacrum of polluted air containing methanol was prepared by bubbling clean air into a container filled with a methanol solution to obtain methanol gas, and then diluting the methanol gas with clean dry air. The initial methanol concentration of the simulated polluted air was controlled by changing the proportion of the bubbling gas and the diluent gas. The reactant mixture was fed to the tube reactor at a flow rate of 4.51 mL min^{-1} and concentration of 5.37 gm^{-3}.

At different reaction temperatures, catalytic reaction for eliminating methanol occurred and the eliminating rate of methanol was determined. The reaction temperature was increased from room temperature to a certain temperature at which methanol was no longer detected in the effluent gases. The concentration of organic compounds of the effluent gases was analyzed on-line by gas chromatography. The inorganic products of the effluent gases were monitored by a 0.2 (wt%) $PdCl_2$ solution and a saturated limewater solution. Blank experiments were carried out in the absence of **1** and **2**.

3. Results and discussion

3.1. *Structure description*

3.1.1. $(C_7N_2H_7)_3(C_7N_2H_6)\cdot PMo_{12}O_{40}\cdot 2H_2O$ (1). Single-crystal X-ray analysis shows that **1** consists of one classical Keggin polyoxoanion, $[PMo_{12}O_{40}]^{3-}$, three $[C_7N_2H_7]^+$,

Table 1. Crystallographic data for **1** and **2**.

Compound	**1**	**2**
Empirical formula	$C_{28}H_{31}O_{42}N_8PMo_{12}$	$C_{35}H_{39}O_{43}N_{10}AsMo_{12}$
Formula weight	2333.86	2513.96
Temperature (K)	293(2)	293(2)
Wavelength (Å)	0.71073	0.71073
Crystal system	Triclinic	Triclinic
Space group	$P\bar{1}$	$P\bar{1}$
Unit cell dimensions (Å, °)		
a	9.8980(4)	12.3353
b	11.2893(4)	13.2649(4)
c	25.8933(9)	20.2878(6)
α	93.307(2)	95.663(10)
β	90.630(2)	100.172(10)
γ	108.330(2)	99.394(10)
Volume (Å^3), Z	2740.68(18), 2	3195.72(17), 2
Calculated density (g·cm^{-3})	2.828	2.613
F(000)	2220	2400
Crystal size (mm^3)	$0.34 \times 0.26 \times 0.20$	$0.36 \times 0.35 \times 0.15$
θ range for data collection (°)	1.90–25.00	2.51–26.00
Description	Block	Block
Color	Dark brown	Red
Limiting indices	$-11 \le h \le 11$; $-13 \le k \le 13$; $-30 \le l \le 30$	$-15 \le h \le 15$; $-16 \le k \le 16$; $-24 \le l \le 25$
R(int)	0.0295	0.0240
$R_1[I > 2\sigma(I)]$	0.0740	0.0329
$wR_2[I > 2\sigma(I)]$	0.1511	0.1236
Parameters	757	910
Goodness-of-fit on F^2	1.037	1.088
Unique data	9432	12,283
Total data	29,290	30,643
Largest difference peak and hole (e . Å^{-3})	2.512 and −1.344	1.037 and −0.979

Table 2. Selected interatomic distances (Å) and angles (°) for **1**.

Atoms	Distance (Å)	Atoms	Angle (°)
P1–O4	1.565(5)	O10–P1–O14	104.2(7)
P1–O5	1.498(3)	O10–P1–O4	112.4(7)
P1–O10	1.471(3)	O14–P1–O4	111.9(8)
P1–O14	1.518(3)	O10–P1–O5	108.8(7)
Mo1–O11	1.643(9)	O14–P1–O5	107.7(8)
Mo1–O40	1.827(10)	O4–P1–O5	111.5(7)
Mo1–O20	1.890(9)	O11–Mo1–O40	101.8(5)
Mo1–O31	1.927(10)	O20–Mo1–O15	85.1(4)
Mo2–O9	1.645(8)	O31–Mo1–O4	59.4(6)
Mo2–O35	1.855(8)	O32–Mo2–O3	102.7(6)
Mo2–O39	1.889(9)	O32–Mo2–O27	100.5(5)
Mo2–O38	1.930(9)	O32–Mo2–O22	101.5(5)
Mo3–O7	1.645(9)	O7–Mo3–O36	104.5(5)
Mo3–O36	1.813(8)	O36–Mo3–O24	90.2(4)
Mo3–O24	1.882(10)	O40–Mo3–O1	95.7(6)

Table 3. Selected interatomic distances (Å) and angles (°) for **2**.

Atoms	Distance (Å)	Atoms	Angle (°)
As1–O17	1.652(3)	O17–As1–O16	109.59(15)
As1–O16	1.653(3)	O17–As1–O39	109.19(15)
As1–O39	1.656(3)	O16–As1–O39	109.76(15)
As1–O21	1.658(3)	O17–As1–O21	109.61(15)
Mo1–O1	1.670(3)	O16–As1–O21	109.34(15)
Mo1–O2	1.844(4)	O39–As1–O21	109.35(15)
Mo1–O3	1.890(3)	O1–Mo1–O2	104.55(17)
Mo2–O10	1.850(3)	O2–Mo1–O7	92.39(14)
Mo2–O6	1.895(3)	O8–Mo1–O21	71.42(12)
Mo2–O9	1.948(3)	O4–Mo2–O9	100.42(15)
Mo3–O6	1.873(3)	O10–Mo2–O9	89.12(14)
Mo3–O11	1.955(3)	O6–Mo2–O9	154.51(14)
Mo3–O17	2.363(3)	O6–Mo3–O3	86.36(15)
Mo4–O23	1.660(3)	O5–Mo3–O12	100.60(16)
Mo4–O22	1.895(4)	O11–Mo3–O17	71.24(12)
Mo4–O11	1.915(3)	O5–Mo3–O17	167.46(14)

one $[C_7N_2H_6]$, and two water molecules (figure 1a). The $[PMo_{12}O_{40}]^{3-}$ anion shows a well-known disordered Keggin structure. The central PO_4 tetrahedron is surrounded by four vertex-sharing Mo_3O_{13} triplets that result from the association of three edgesharing MoO_6 octahedra. The P–O distances are 1.471(13)–1.565(15) Å and O–P–O angles 104.2(7)–112.4(7)°. The Mo–O bonds can be divided into three groups [16]: (i) Mo–O_t (terminal), 1.658(4)–1.672(6) Å, mean 1.665 Å; (ii) Mo–O_b (bridge), 1.861(5)–1.955(7) Å, with an average bond length of 1.901 Å; (iii) Mo–O_c (central), 2.422(7)–2.496(7) Å, mean 2.479 Å. Comparing the Mo–O bonds with those of $H_3[PMo_{12}O_{40}] \cdot 13$–$14\ H_2O$, the Mo–$O_c$ and Mo–O_t bonds show an obvious increase, but the Mo–O_b bonds do not change. The results indicate that the static electronic interaction between the $[PMo_{12}O_{40}]^{3-}$ and discrete $[C_7N_2H_7]^+$ are relatively weak. The Mo–O_c–Mo and Mo–O_b–Mo angles are 92.5(8)–96.3(7)° and 134.8(15)–142.0(10)°, respectively, exhibiting that all the Mo atoms are in distorted octahedral geometry.

In the crystal, there exist intramolecular hydrogen bonds and intermolecular hydrogen bonds (figure 1b). Benzimidazole as hydrogen-bond donor provides H1A–O14 of phosphomolybdic heteropolyanion (d(N1 $\cdots$ O14) = 2.805(16) Å, ∠N1–H1A $\cdots$ O14 = 161°, etc.), forming an intramolecular hydrogen bond, while benzimidazole as hydrogen-bond donor of H2A–O16i (d(N2 $\cdots$ O16i) = 3.074(17) Å, ∠N2–H2A $\cdots$ O16i = 122°, etc.) of the adjacent phosphomolybdic heteropolyanion (i: $2-x$, $1-y$, $1-z$) formed a non-classical intermolecular hydrogen bond. Face-to-face π–π stacking interactions among benzimidazole molecules stabilize the molecular structure. The centroid distance of 3.941(10) Å between N(1)– and N(5)– rings; the centroid distance of 4.141(11) Å, dihedral angle of 2.488°, and upright distances of 3.975 Å and 4.167 Å between the N(3)– and N(7)– rings; the centroid distance of 3.890(5) Å, dihedral angle of 2.644°, and upright distances of 3.796 Å and 3.955 Å between N(5)– and symmetry related N(7)–rings ($1-x$, $-y$, $-z$) clearly suggest the existence of aromatic π–π stacking interactions. The π–π stacking interactions and hydrogen bonds endow **1** with an interesting 3-D supramolecular array (figure 1c).

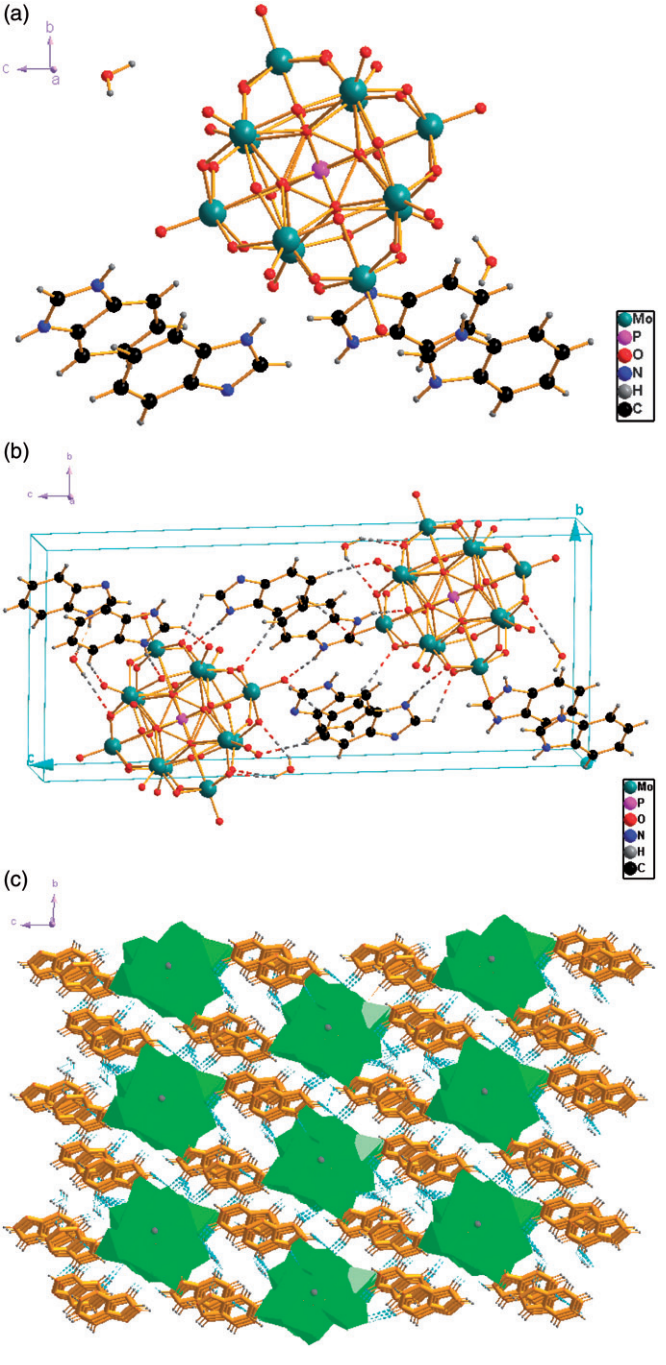

Figure 1. (a) Drawing of the asymmetric unit of **1**, (b) packing diagram of **1**, and (c) polyhedral representation of the 3-D structure by hydrogen bonds and π–π stacking interaction along the *a*-axis in **1**.

3.1.2. $(C_7N_2H_7)_3(C_7N_2H_6)_2 \cdot AsMo_{12}O_{40} \cdot 3H_2O$ (2). As shown in figure 2(a), a molecular unit of **2** consists of one polyoxoanion $[AsMo_{12}O_{40}]^{3-}$, three $[C_7N_2H_7]^+$ cations, two $[C_7N_2H_6]$, and three water molecules. $AsMo_{12}O_{40}^{3-}$ exhibits the classical α-Keggin-type structure [17]: twelve MoO_6 octahedra present in four Mo_3O_{13} groups and surrounded by a AsO_4 tetrahedron. For the AsO_4 tetrahedron, the As–O bond lengths are 1.652(3)–1.658(3) Å with average of 1.655 Å, while the O–As–O angles vary from 109.19(15) to 109.76(15)°. The Mo–O_t, Mo–$O_{b,c}$–Mo, and Mo–O_c bond distances are 1.656(3)–1.670(3), 1.844(3)–1.995(9), and 2.340(3)–2.364(3) Å with average lengths of 1.662, 1.921, and 2.356 Å, respectively. The O–Mo–O angles fall in the range of 71.42(12)–171.61(15)°. These data reveal that the polyanion of **2** is slightly distorted.

The extensive hydrogen bonds with their surrounding heteropolyanions and benzimidazoles result in an intricate hydrogen-bonding supramolecular 2-D network (figure 2b). The benzimidazole in one unit cell coincides with the adjacent one, which brings about π–π stacking interactions with shortest C–C distance of 3.594(16) Å. With both the hydrogen bonds and π–π stacking interactions, **2** forms a 3-D organic–inorganic supramolecular network (figure 2c).

3.2. *Characterization of compounds*

3.2.1. IR spectra. IR spectra of **1** and **2** were tested before and after the catalytic reaction and did not show a change. The IR spectrum shows strong absorptions at 1148–2980 cm^{-1} assigned to the characteristic vibration of benzimidazole. Peaks at 3140–3500 cm^{-1} are ascribed to ν(O–H) and ν(N–H). Both the compounds give characteristic peaks of Keggin anion at 1057, 960, 867, and 789 cm^{-1} for **1**, 961, 892, 844, and 771 cm^{-1} for **2**, attributed to ν(X–O_c), ν(Mo–O_t), ν(Mo–O_c), and ν(Mo–O_b), respectively (X = P and As). Comparing the IR spectrum of **1** with that of $H_3PMo_{12}O_{40} \cdot nH_2O$ (ν = 1064 (P–O_c), 963 (Mo–O_t), 870 (Mo–O_c), 782 (Mo–O_b) cm^{-1}) [18], the vibrational bands of the P–O_c, Mo–O_c, and the Mo–O_t bond have a small red-shift, while the vibrational bands of Mo–O_b are blue-shifted. This demonstrates that the P–O_c, Mo–O_c, and the Mo–O_t bonds become weaker, and the Mo–O_b bonds become stronger in **1**. Comparing the IR spectrum of **2** with that of $Li_3AsMo_{12}O_{40} \cdot xH_2O$ (ν = 963 (As–O_c), 895 (Mo–O_t), 846 (Mo–O_c), 773(Mo–O_b) cm^{-1}) [19], all vibrational bands of the bonds in the Keggin structure have a small red-shift. The IR spectrum indicates interactions between $[XMo_{12}O_{40}]^{3-}$ (X = P and As) and $[C_7N_2H_7]^+$ in the solid state.

3.2.2. TG analyses. The TG-DTA analyses of **1** and **2** were performed from 25°C to 700°C. From 320°C to 550°C, there are two exothermic peaks at 369.8°C and 408.9°C for **1** and 341.7°C and 412.9°C for **2**, accompanied by considerable weight loss, which correspond to release of benzimidazole and decomposition of $(XMo_{12}O_{40})^{3-}$ (X = P and As) polyoxoanions. The final residue, whose total weight loss is 25.28% (Calcd 24.81%) for **1** and 30.52% (Calcd 31.27%) for **2**, is MoO_3, which is verified by IR spectra.

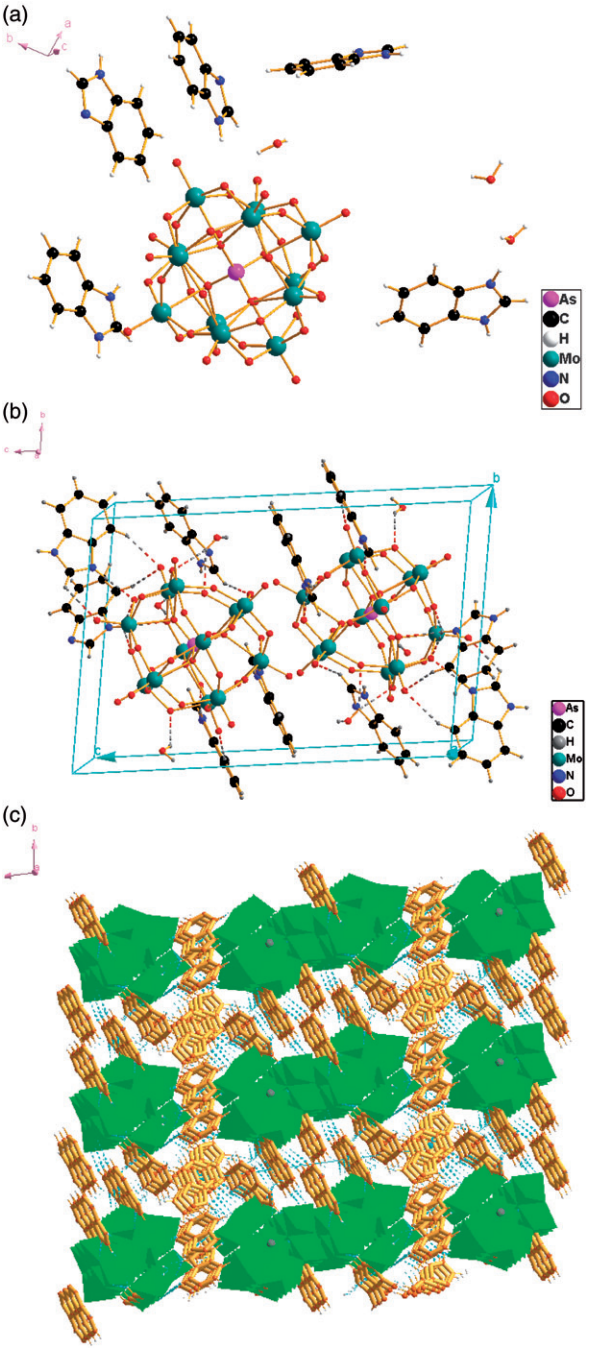

Figure 2. (a) Drawing of the asymmetric unit of **2**, (b) packing diagram of **2**, and (c) polyhedral representation of the 3-D structure by hydrogen bonds and π–π stacking interaction along the *a*-axis in **2**.

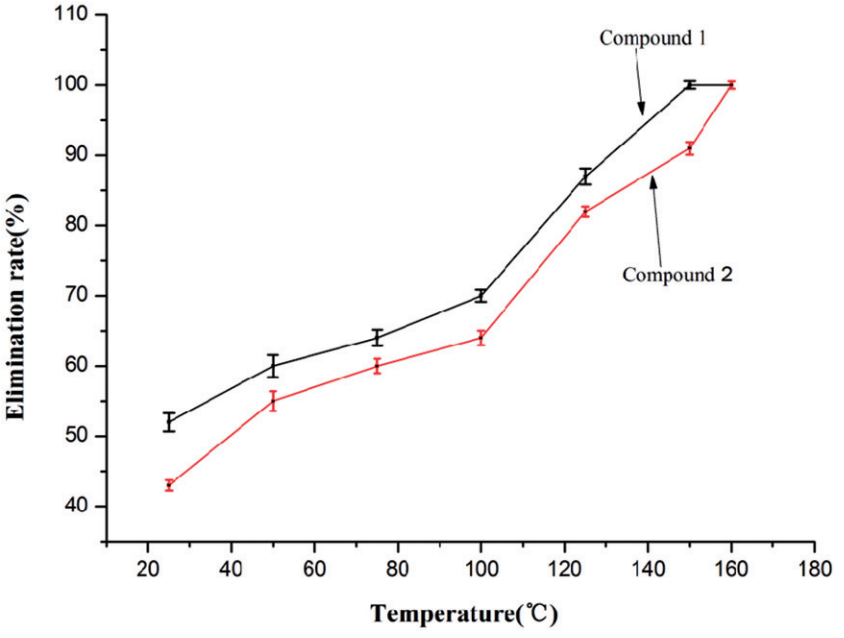

Figure 3. Curves of methanol elimination rate *vs.* temperature for **1** and **2**.

3.3. *Catalytic reaction*

Blank experiments show that methanol in a simulacrum of polluted air was not eliminated oxidatively without **1** or **2** as a catalyst. From the results of the effluent gases after catalytic reaction, there is no new peak in the GC diagram, indicating no new organic compounds formed; lime saturated water formed precipitate and the color of the 0.2% $PdCl_2$ solution did not change, indicating that there was CO_2 but no CO. Products of the elimination of methanol were CO_2 and H_2O. The temperature of catalytic reaction was 25–150°C, lower than the decomposition temperature of **1** and **2**. The relationship between the elimination rate and temperature is shown in figure 3.

In Chinese environment quantity standards (TJ36-79), the maximum allowable concentrations of methanol in air of residential and workshop areas are 0.003 g m^{-3} and 0.05 g m^{-3}, respectively. The catalytic test results show that methanol of concentration 5.37 g m^{-3} at a flow velocity of 4.41 mL min^{-1} was completely eliminated at 150°C over 0.20 g of **1** as catalyst (160°C for **2**). This methanol concentration is greater than the maximum concentration allowed by the national emission standards. From figure 3, **1** has a slightly higher methanol elimination rate at the same temperature and lower complete elimination temperature than **2**. The mean difference of elimination rate between **1** and **2** is 7.6%. The difference of the molar amount between both is 7.12%. For the same weight, there are less molecules of **2** compared to **1**, so there are less active sites. This could contribute to the lower elimination rate of **2**. It may also be attributed to different intensities and numbers of hydrogen bonds of **1** and **2**, which show different adsorption ability, affecting the catalytic activity.

4. Conclusions

Two new organic–inorganic supramolecular compounds based on Keggin polyoxotungstates, $(C_7N_2H_7)_3(C_7N_2H_6)\cdot PMo_{12}O_{40}\cdot 2H_2O$ (**1**) and $(C_7N_2H_7)_3(C_7N_2H_6)_2\cdot AsMo_{12}O_{40}\cdot 3H_2O$ (**2**), have been synthesized by a hydrothermal method and their structures elucidated by single-crystal X-ray diffraction. The two compounds contain a large number of hydrogen bonds and π–π stacking interactions, giving 3-D organic–inorganic supramolecular networks with alternating layers of Keggin anions and benzimidazole molecules.

Research studies concerning POMs on catalysis involving $[Hmim]_3PW_{12}O_{40}$ (mim = methylimidazole) as a heterogeneous catalyst for alcohol oxidation with hydrogen peroxide [20] and Anderson-type POMs $(H_3O)[(3\text{-}C_5H_7N_2)_2(Cr(OH)_6Mo_6O_{18})]\cdot 3H_2O$ have catalytic activities for oxidation of acetone [21]. There are few papers about organic–inorganic hybrid Keggin-type POMs used for catalysis eliminating VOC. Complexes **1** and **2** have good catalytic oxidation activity for eliminating methanol. Methanol concentration of $5.37\,g\,m^{-3}$ was completely eliminated at 150°C for **1** and 160°C for **2** over 0.20 g of compound as catalyst, which is far greater than the national discharge standard concentration of methanol. Especially without any activation treatment, the two compounds show good catalytic activity, which is rare in the class of catalysts, pointing to potential applications in catalytic oxidation.

Acknowledgments

This project was supported by the Hunan Provincial Science and Technology Plan Projects of China and Key Laboratory of Theoretical Chemistry and Molecular Simulation of Ministry of Education, Hunan University of Science and Technology.

References

[1] C.L. Hill. *Chem. Rev.*, **98**, 1 (1998).
[2] Q. Chen, C.L. Hill. *Inorg. Chem.*, **35**, 2403 (1996).
[3] Y. Xu, H.G. Zhu, H. Cui, X.Z. You. *Chem. Commun.*, 787 (1999).
[4] I.V. Kozhevnikov. *Chem Rev.*, **98**, 171 (1998).
[5] M. Mizuno, M. Misono. *Chem Rev.*, **98**, 199 (1998).
[6] Y.H. Guo, Y.H. Wang, C.W. Hu, Y.H. Wang, E.B. Wang. *Chem. Mater.*, **12**, 3501 (2000).
[7] T. Akutagawa, D. Endo, H. Imai, S. Noro, L. Cronin, T. Nakamura. *Inorg. Chem.*, **45**, 8628 (2006).
[8] J.A.F. Gamelas, A.M.V. Cavaleiro, E.D.M. Gomes. *Polyhedron*, **21**, 2537 (2002).
[9] M.P. Shores, L.G. Beauvais, J.R. Long. *J. Am. Chem. Soc.*, **121**, 775 (1999).
[10] C.R. Kagan, D.B. Mitzi, C.D. Dimitrakopoulos. *Science*, **286**, 945 (1999).
[11] P. Shringarpure, B.K. Tripuramallu, K. Patel, A. Patel. *J. Coord. Chem.*, **64**, 4016 (2011).
[12] M.L. Wei, H.H. Li, G.J. He. *J. Coord. Chem.*, **64**, 4318 (2011).
[13] G.M. Sheldrick. *SADABS, Program for Empirical Absorption Correction of Area Detector Data*, University of Göttingen, Göttingen, Germany (2003).
[14] G.M. Sheldrick. *SHELXS-97, Program for the Solution of Crystal Structures*, University of Göttingen, Göttingen, Germany (1997).
[15] G.M. Sheldrick. *SHELXL-97, Program for the Refinement of Crystal Structures*, University of Göttingen, Göttingen, Germany (1997).

[16] P.P. Zhang, J. Peng, A.X. Tian, H.J. Pang, Y. Chen, M. Zhu, D.D. Wang, M.G. Liu, Y.H. Wang. *J. Coord. Chem.*, **63**, 3610 (2010).
[17] M.T. Pope. *Heteropoly and Isopoly Oxometalates*, Springer, Berlin (1983).
[18] S. Lin, Y.Z. Yea, X.F. Zhang, C.L. Liu. *Transition Met. Chem.*, **31**, 760 (2006).
[19] C. Rocchiccioli-Deltcheff, M. Fournier, R. Franck, R. Thouvenot. *Inorg. Chem.*, **22**, 207 (1983).
[20] X.J. Lang, Z. Li, C.G. Xia. *Synth. Commun.*, **38**, 1610 (2008).
[21] Z.S. Peng, C.L. Zhang, X.M. Shen, Q. Deng, T.J. Cai. *J. Coord. Chem.*, **64**, 2848 (2011).